ARCHIVES OF ACOUSTICS
23, 4, 499–511 (1998)

APPLICATION OF THE FRACTAL ANALYSIS IN THE SEA BOTTOM RECOGNITION

Z. ŁUBNIEWSKI and A. STEPNOWSKI

Technical University of Gdańsk
Acoustics Department
(80-952 Gdańsk, Narutowicza 11/12)
e-mail: lubniew@eti.pg.gda.pl, astep@pg.gda.pl

The paper proposes a newly developed simple method of the sea bottom typing using elements of fractal analysis. The fractal dimension was calculated as a box dimension for sampled envelopes of echo signals from four types of sea bottom recorded during mobile acoustic surveys carried out in Lake Washington. The histograms of obtained box dimension values for particular bottom types as well as scatter diagrams in box dimension-echo energy parameter space were constructed and analysed. The obtained results show that this simple method can be used both alone and combined with other methods for on board sea bed recognition in real time with accuracy similar to that of other methods.

1. Introduction

The problem of a proper sea bottom identification is important in many fields, for instance in hydrography, marine engineering, environmental sciences, fisheries and other domains. Acoustic methods of sea bottom typing, which use the information retrieved from the bottom echo, have advantages over the other methods (e.g. geological cores or remotely operated vehicles with TV cameras), as being faster, non-invasive and more cost effective.

In general, the following approaches are used in the acoustic methods of bottom typing:

- measurement of energy ratio of the first and second bottom echo ("Roxann" method) [3] or division of the first echo signal [1],
- comparison of the actual cumulative echo envelopes with theoretical patterns [7],
- analysis of a set of values of acoustic and statistical parameters of the echo envelope using cluster analysis [12, 13] or artificial neural networks [4, 8],
- using parametric sources and wideband "chirp" signals [2, 4].

All acoustic methods of bottom identification are based on the assumption, that the received echo pulse contains the significant and possible to retrieve information about the bottom characteristics. The authors have developed the simple method in which fractal dimension of an echo envelope is used as a signature of the bottom type. It is known that the surface of sea bottom is one of examples of a fractal structured object in

nature [9]. Taking this into consideration we made an implicit assumption that fractal structure of the bottom is transferred onto its image observed in the reduced form as an envelope of sonar echo. The fractal dimension of the bottom surface can be treated as a measure of its complexity and roughness, which is correlated with hardness of the sediment, as the harder bottom, the more irregular, corrugated shape it has. That is why we predicted that the envelopes of echoes from harder bottom would have greater fractal dimension values than those of echoes from softer bottom.

2. The outline of the fractal analysis

It was found that the shapes and structures of many objects in nature usually show no regularities that are characteristic of simple figures, which can be easily described in terms of the Euclidean geometry. That is why this kind of geometry is not the most adequate tool for describing such objects. On many occasions, however, nature has proved to accommodate various types of elements with the fractal structure, e.g. the structure of plants' leaves, corrugated sea surface or bottom surface [9], which suggests that fractal analysis methods are the proper methods for studying and describing such elements.

The Koch snowflake (Fig. 1a) could be an example of a fractal figure. It is defined as a limit of the sequence of simple iterative steps: Starting with the equilateral triangle, each consecutive stage is constructed by replacing each line segment with copy of the broken line of the following shape: $\_/\!\!\backslash\_$. In the random version of the Koch snowflake (Fig. 1b), in every stage the replacement by $\_/\!\!\backslash\_$ or $\backslash\!\!/$ may be made, with probability of 0.5 for each case. The Cantor set [9] can be another example of the fractal structure.

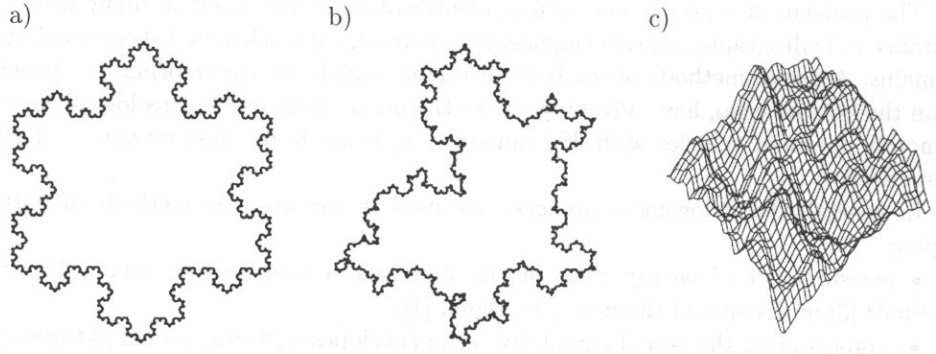

Fig. 1. The examples of fractal 2D and 3D figures; a) the regular Koch snowflake, b) the randomized Koch snowflake, c) fractal surface.

Fractal sets are defined as scale-invariant (self-similar) geometric objects. A geometric object is called scale-invariant, if it can be written as a union of rescaled copies of itself. Regular fractals, such as the Koch snowflake, Cantor set or Sierpiński triangle, demonstrate exact self-similarity [9, 11]. Random fractals show a weaker, statistical version of self-similarity.

The interesting feature of fractal figures is its similarity to some objects occurring in nature. For instance, the random version of the Koch snowflake from Fig. 1b could remind a mountain lake, and the computer generated fractal surface (Fig. 1c) has the shape similar to that of corrugated sea surface or sea-bed.

To be able to investigate and describe real objects in nature with use of the fractal analysis, one should have a method of measuring the magnitude of their dimensions and comparing them. Standard methods, that consist of measuring of length or area of 1D and 2D figures, are not appropriate here. The Koch snowflake, for instance, has an area equal to zero, but its length tends to infinity when the size of the measuring step tends to 0.

One of the used fractal dimensions, so-called Hausdorff dimension [9, 11] may be the solution to this problem, as it can be used as a measure of many very general sets, including fractals. The Hausdorff dimension of a subset X of Euclidean space is defined as a limit

$$D = \lim_{r \to 0} \frac{-\log N(r)}{\log r}, \tag{1}$$

where $N(r)$ denotes the smallest number of open balls of radius r needed to cover subset X; an open ball $B(p,r) = \{x : \text{dist}\,(x,p) < r\}$, where $\text{dist}\,(x,p)$ is the distance between points x and p. For example, it could be shown [9], that the Koch snowflake has the Hausdorff dimension equal to $\log 4/\log 3 \approx 1.262$.

It is easy to see that the dimension defined by formula (1) measures of the complexity of a given figure. In the case of a sea bottom echo envelope, it should be an indicator of the complexity or variability of this waveform, which may imply its use as a signature of the type of investigated sea-bed.

3. Materials and methods

The bottom echoes data we used to calculate the fractal dimension were recorded during acoustic surveys on Lake Washington with the use of digital DT4000 BioSonics echosounder with two operating frequencies: 38 and 120 kHz. Simultaneously the current position of the research vessel has been controlled and recorded using the GPS system. Data acquisition was performed both while the vessel was moving along the selected transects, and while the ship was anchored. In each case the type of sea bottom in the given water region was known from ground samples taken by divers. This enabled a validation of the developed and applied method of bottom typing. The length of the sounding pulse of the echosounder was 0.4 ms and the frequency of sampling of the echo envelope at the echosounder output was equal to 41.66 kHz.

It is not easy to calculate the fractal dimension of a figure following the definition of the Hausdorff dimension (1). Therefore we decided to use the box dimension [9], that can replace the Hausdorff dimension for many sets, including shapes of our echo pulses. The box dimension of a plane figure of investigated echo waveforms is defined as follows. Let $N(\Delta s)$ denote the number of boxes in a grid of the linear scale Δs which meet the

set X on a plane. Then X has a box dimension

$$D = \lim_{\Delta s \to 0} \frac{-\log N(\Delta s)}{\log \Delta s}. \tag{2}$$

The method of evaluating the box dimension of a bottom echo envelope is explained in Fig. 2. The grid of square boxes of side Δs is superimposed on the graph of echo envelopes and the number of boxes which consist of the fragments of the envelope graph is counted and denoted as $N(\Delta s)$. It must be pointed out, that here we cannot use the accurate definition of box dimension with limit given by formula (2), because a digitized echo pulse consists of a finite set of straight sections and it is not a real fractal. That is why one would always obtain the box dimension value equal to 1. However, it is possible to approximately evaluate this dimension for such a figure calculating it not as a limit, but assuming Δs to have a finite fixed value:

$$\widetilde{D}_{\text{box } \Delta s} = \frac{-\log N(\Delta s)}{\log \Delta s} \tag{3}$$

or substituting Δs by $1/N_s$, where N_s is both horizontal and vertical number of boxes in the grid:

$$\widetilde{D}_{\text{box } N_s} = \frac{\log N(N_s)}{\log N_s}. \tag{4}$$

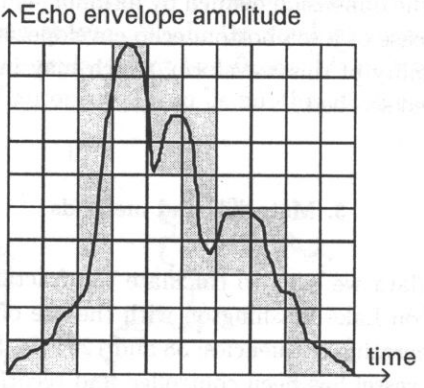

Fig. 2. Illustration of the box dimension evaluation. In the considered case, $\Delta s = 0.1$, $N_s = 10$, $N(\Delta s) = 30$.

We evaluated the box dimension of the echo pulses envelopes acquired during the surveys using the above concept with $\Delta s = 1/36$, after normalizing each echo pulse to the standard length and height. Additionally, we tested a modified version of the box dimension evaluation procedure, which has two following differences from the one discribed above.

Firstly, we used the grid of rectangular, instead of square boxes, what meant that the numbers of boxes in the grid along the horizontal (N_{sx}) and vertical (N_{sy}) axis were not equal, as we wanted to investigate the irregularity, or complexity, of an echo

envelope using different horizontal and vertical scale. In such a case, the formula (3) or (4) used for evaluating the box dimension had to be modified, to take into account the difference between N_{sx} and N_{sy}. Following the principle, that the least irregular, straight horizontal line – the graph of a constant function – has the box dimension equal to 1 and such the line would cause N_{sx} rectangular boxes of the grid to be marked as dark, and the second principle, that the most composed line, which would cause all of boxes $(N_{sx} \cdot N_{sy})$ to be darked, has the box dimension approximately equal to 2, we derived the more general formula for the box dimension:

$$\widetilde{D}_{\text{box}\,N_{sx},N_{sy}} = \frac{\log\left[N(N_{sx},N_{sy}) \cdot \dfrac{N_{sy}}{N_{sx}}\right]}{\log N_{sy}}. \tag{5}$$

The second modification in procedure of calculating the box dimension of echo envelopes was made to avoid normalizing, what means enlarging or squeezing all echo pulses to one standard length, what could affect the final results. Because of differences in length of particular echo pulses, we applied the concept of moving window of fixed length W samples, not greater than length of the shortest echo pulse in the data set. For each pulse we evaluated the box dimension as an average of the box dimensions calculated for parts of signal with length W, sequentially being chosen from the whole pulse:

$$\widetilde{D}_{\text{box}} = \frac{1}{N-W+1} \sum_{i=1}^{N-W+1} \widetilde{D}_{\text{box}}(i, i+W-1), \tag{6}$$

where N is the whole echo pulse length in samples and $\widetilde{D}_{\text{box}}(i,j)$ denotes the box dimension calculated for a part of the pulse starting at i-th sample and ending at j-th sample. We used the window of $W = 48$ samples in length.

Three sets of data for testing the proposed sea bottom typing method were used:

1) echoes recorded on the anchored ship, at echosounder frequency 120 kHz,

2) echoes recorded on the anchored ship, at echosounder frequency 38 kHz,

3) echoes recorded during moving along transects, at echosounder frequency 120 kHz.

Each of these sets contained digitized envelopes of echo pulses from four different types of sea bottom: soft mud, soft sand, hard sand and rock. There were more than 600 echoes from each type of bottom in each data set. Before calculations, only 10% of pings of the highest amplitude were selected from each data set in order to take into account only the echoes from pulses with the most likely normal incidence to the bottom (and drop the others), reducing the effect of a ship's pitching and rolling in this way.

The amplitude threshold used for the analysed signals was −70 dB. The box dimension was calculated for each echo pulse separately, and histograms of its values for each type of bottom were constructed and analysed. Additionally, other echo pulse parameters, connected with the echo energy, were calculated in some cases and scatter diagrams with points in the 2-dimensional parameter space were constructed.

4. The results of the box dimension evaluation

Figures 3a, 3b, 4 and 5 show the histograms of box dimension values obtained for echo pulses for four types of bottom. Figures 3a and 3b show the results obtained for the first

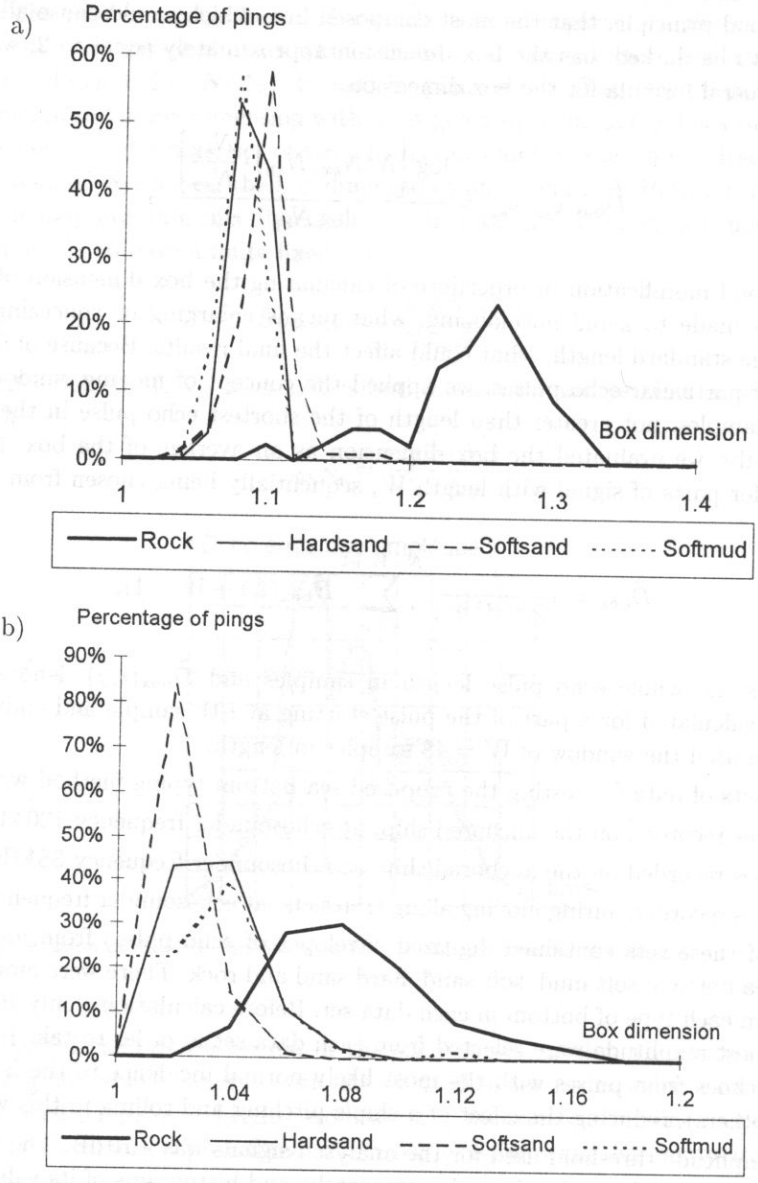

Fig. 3. a. The histogram of the box dimension evaluated from bottom echo pulses recorded on an anchored ship at frequency 120 kHz (first method – square boxes). b. The histogram of the box dimension evaluated from bottom echo pulses recorded on an anchored ship at frequency 120 kHz (second method – rectangular boxes and moving window).

data set, Fig. 4 the results for the second data set, and Fig. 5 for the third. Figures 3a, 4 and 5 present histograms of the box dimension obtained by applying the first method, using the grid of square boxes and without applying the moving window. Figure 3b presents the results obtained by applying the second, modified method of box dimension evaluation, using rectangular boxes ($N_{sx} = 48$, $N_{sy} = 16$) and the moving window. As one can see by comparing Fig. 3a and Fig. 3b, there are no significant differences between the results of both methods, as far as the shapes of histograms and mutual relations between distributions of box dimension of echoes from particular types of bottom are concerned. We found this also true for two other sets of data, so we decided to stay with the first method results for further analysis. However, the visible differences between absolute values of box dimension obtained in the first and second method (Fig. 3a and Fig. 3b) need the explanation. This difference is the result of applying grids with boxes of different sizes in each of these two cases, what certainly cannot affect the results of box dimension calculation for mathematical, "real" fractal figures, but can cause differences between obtained values in the case of an echo envelope which is in fact a broken line and not a fully featured fractal.

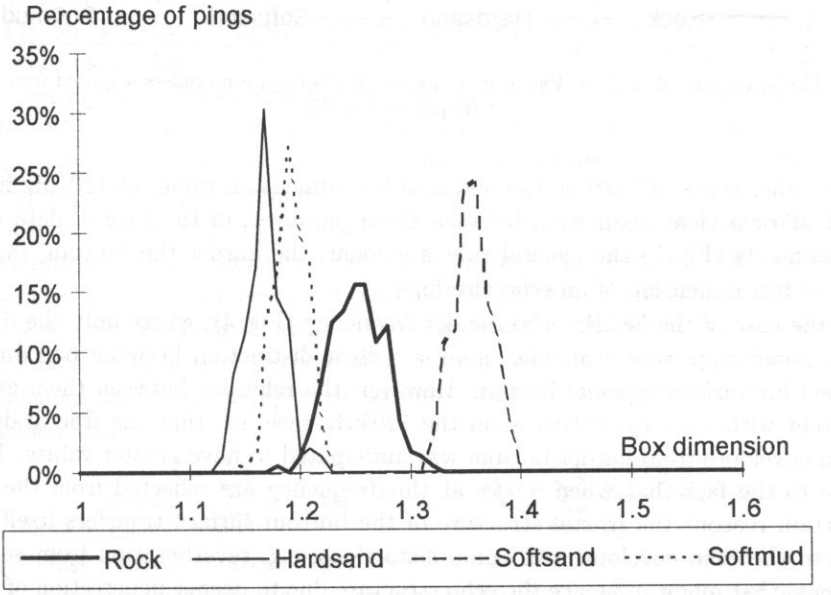

Fig. 4. The histogram of the box dimension evaluated from bottom echo pulses recorded on an anchored ship at frequency 38 kHz.

The presented histograms of box dimension values show that in the case of 120 kHz frequency of the echosounder (Fig. 3) there is a clear difference between the values of the box dimension for a rocky bottom and for the other types of seabed, especially for the data collected on the anchored ship. In the case of rock the box dimension values are significantly greater ($1.2 \div 1.3$ vs. ca 1.1 for the other types of bottom), what is consistent with expectations, because the surface of rocky bottom is more corrugated and irregular.

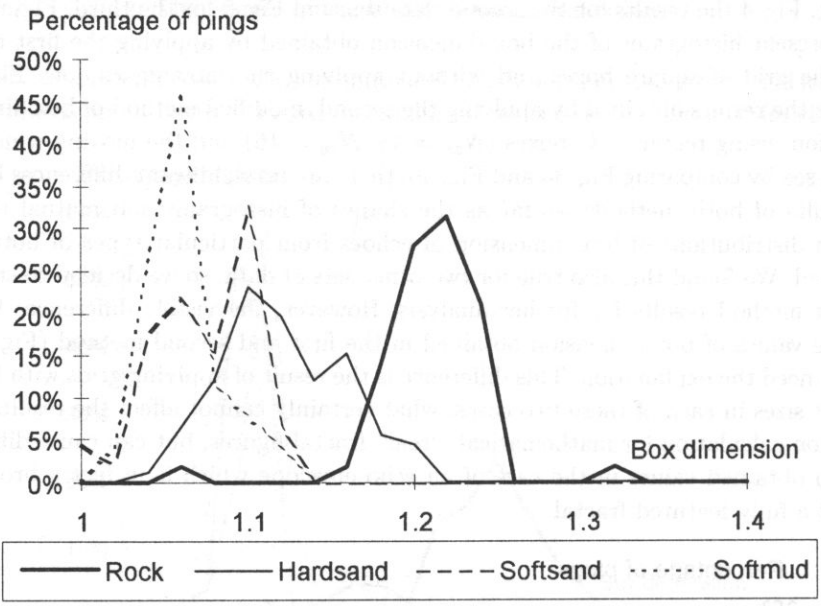

Fig. 5. The histogram of the box dimension evaluated for bottom echo pulses acquired from transects at frequency 120 kHz.

For the other types of bottom, the obtained box dimension values at 120 kHz frequency do not allow a clear distinction between them, however, in the case of data obtained from transects (Fig. 5) the general rule is evident: the harder the bottom, the greater values of box dimension of an echo envelope.

In the case of the 38 kHz echosounder frequency (Fig. 4), where only the data from the anchored ship were available, there is a clear distinction between box dimensions obtained for various types of bottom. However, the relations between them are not as consistent with the expectation as in the 120 kHz case, i.e. that the fractal dimension of echo envelopes from harder bottom was anticipated to have greater values. This may be due to the fact that when pulses at this frequency are reflected from the bottom, for certain reasons the fractal structure of the bottom surface transfers itself onto its image in the echo envelope with some distortions, e.g. reverberation from subbottom sediments that might influence the echo structure due to deeper penetration of pulses of lower frequency.

5. Combining the box dimension parameter with the echo energy. Application of the minimum distance classifier

The authors predicted that performance of the described fractal dimension method of sea bottom typing might be improved by combining it with other methods, using the different parameters of received bottom echo. To test this prediction, besides the

evaluation of box dimension of an echo envelope, the parameters containing information about the echo energy were calculated. Subsequently, the scatter diagrams of data points in the two parameter space were constructed, in similar way as in Roxann or the first echo division method [1, 3]. Three parameters connected with the echo energy were calculated for each pulse, viz.:

- the energy of the attack phase of an echo E_1', which may be treated as an indicator of the hardness of bottom,
- the energy of the decay and release phases of an echo E_1 – the indicator of the roughness of bottom,
- the total energy of the first echo $E = E_1' + E_1$ [1]:

$$E_1' = \int_a^{\tau} V^2(t)\,dt, \qquad E_1 = \int_{\tau}^{b} V^2(t)\,dt, \qquad E = \int_a^{b} V^2(t)\,dt, \tag{7}$$

where V – echo voltage, a – start point of an echo pulse, b – end point of an echo pulse, τ – position of the maximum echo amplitude.

The scatter diagrams of the echoes in the 2-dimensional parameter space (E, D_{box}) are shown in Fig. 6: the space of parameter E_1' vs. D_{box} in Fig. 6a and the space of E vs. D_{box} in Fig. 6b. The data from the anchored ship acquired at the echosounder frequency 120 kHz were used. One can see on the both diagrams, that while the box dimension allows to distinguish between rock and the other types of bottom, the value of the second parameter, E_1' or E, could be in this case used for discrimination between hard sand and mud. These diagrams show that using more than one parameter of an echo improves the bottom typing method performance.

In addition, the authors constructed and tested an automatic procedure of bottom type recognition – the 2-dimensional minimum distance classifier [10] based on values of box dimension and the total energy of echo pulses, which used the data from the scatter diagram in Fig. 6b. In the first stage of the classification procedure, 70% of echo pulses from each bottom type were selected as a training set and the average values of their box dimensions and total energy were calculated as co-ordinates of cluster centers in a 2-dimensional space:

$$\overline{D}_{\text{box}\,k} = \sum_{m=1}^{M_k} D_{\text{box}\,km} \Big/ M_k\,, \qquad \overline{E}_k = \sum_{m=1}^{M_k} E_{km} \Big/ M_k\,, \tag{8}$$

where k – class number (bottom type), m – number of echo pulse within a given class, $D_{\text{box}\,km}$ – box dimension value of a given echo pulse, E_{km} – total energy of a given echo pulse, M_k – number of echoes in a given class in entire training set (70% of all echoes in a class), $\overline{D}_{\text{box}\,k}$ – average value of $D_{\text{box}\,km}$ for a given class in the training set, $\overline{E}_k$ – average value of E_{km} for a given class in the training set.

Subsequently, the procedure of classification was carried out, following the rule of minimum distance from a cluster center i.e. each echo pulse was assigned to that class, for which the distance between the echo point in the 2-dimensional (E, D_{box}) space and the cluster center of that class was minimal, what can be expressed as:

$$C_{km} = l\colon \text{dist}\,(X_{km}, \overline{X}_l) = \min_{\kappa=1\ldots K} \left(\text{dist}\,(X_{km}, \overline{X}_\kappa)\right), \tag{9}$$

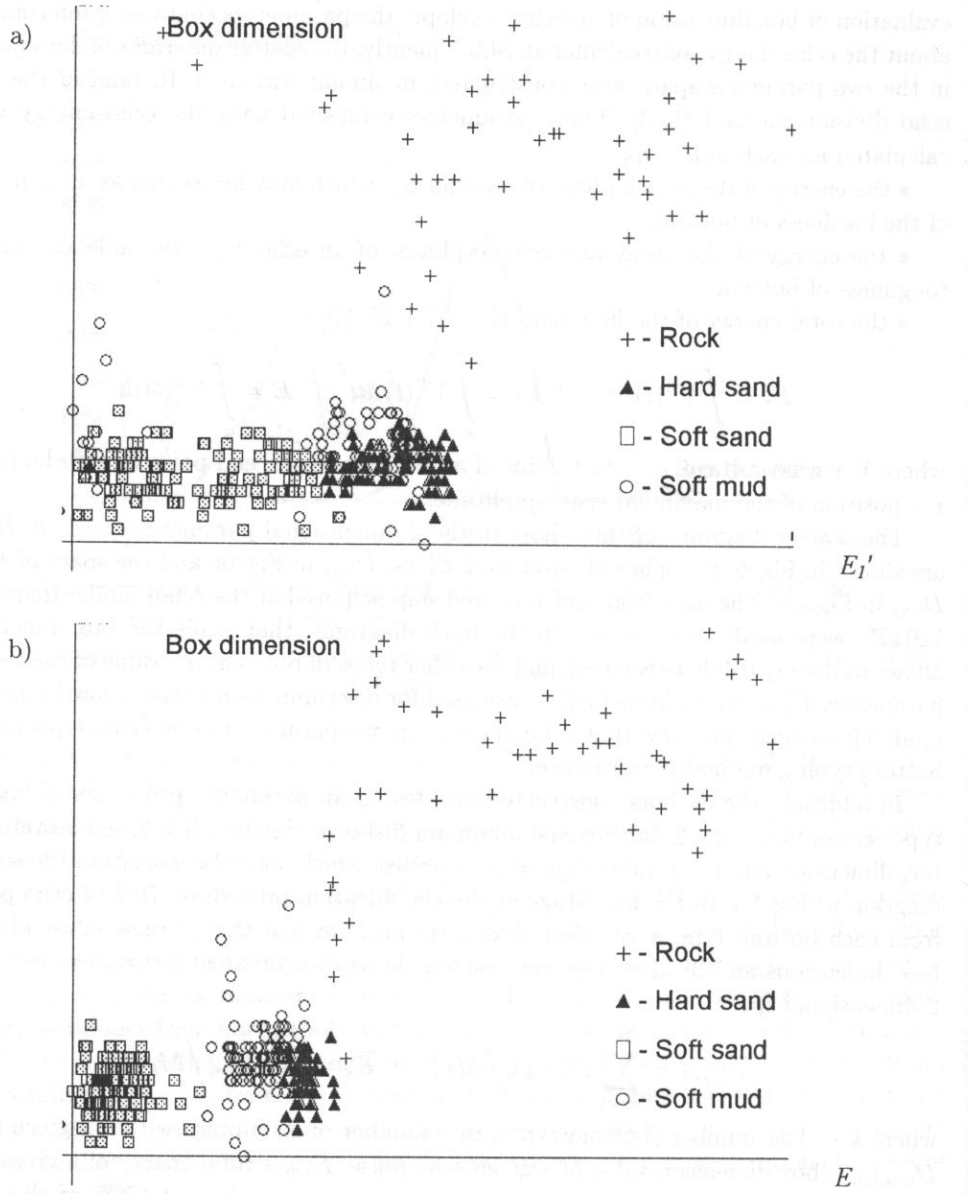

Fig. 6. a. Scatter diagrams of bottom echoes from anchored ship for frequency 120 kHz in the 2-dimensional space of parameters E_1' and D_{box}. b. Scatter diagrams of bottom echoes from anchored ship for frequency 120 kHz in the 2-dimensional space of parameters E and D_{box}.

where K – number of classes, C_{km} – class number assigned to the pulse, X – point in the 2-parameter space corresponding to an echo or to a cluster center: $X(E, D_{\text{box}})$.

The standard formula for calculating the distance between two points in the parameter space (E, D_{box}) was slightly modified and each square of the difference of points'

co-ordinates was additionally divided by the variance of a given parameter in the training set:

$$\text{dist}\,(X_{km}, \overline{X}_l) = \sqrt{\left(E_{km} - \overline{E}_l\right)^2 / \sigma^2_{E_l} + \left(D_{\text{box}\,km} - \overline{D}_{\text{box}\,l}\right)^2 / \sigma^2_{D_{\text{box}\,l}}}, \tag{10}$$

where $\sigma^2_{E_l}$ and $\sigma_{D_{\text{box}\,l}}$ denote the variance of energy and box dimension values respectively within l-th class in the training set.

Additionally, in the preliminary stage of the classification procedure, all values of both parameters E and D_{box} were linearly mapped to [0, 1] interval, to avoid the influence of great differences in ranges of E and D_{box}.

The classification results are shown in Table 1 in a form of the percentage values in confusion matrix.

Table 1. Confusion matrix for the tested minimum distance classifier based on values of box dimension and total energy of echo pulses.

True class	Assigned class (%)			
	Soft mud	Soft sand	Hard sand	Rock
Soft mud	**100**	0	0	0
Soft sand	0	**92.59**	7.41	0
Hard sand	0	27.59	**72.41**	0
Rock	0	7.69	0	**92.31**
Total percentage of correct assignments: 89.32%				

The classification results are satisfactory as the particular classes are quite well separable, what is easily to seen in Fig. 6b. In general, only echoes from soft and hard sand were confused, as the result of the E and D_{box} parameters distributions overlap for these types of bottom.

6. Inverse filtering

An extension of the described method could be an application of the deconvolution of the spatio-temporal scattering impulse response of seabed from bottom echo, before the fractal dimension calculation. In general, the spatio-temporal acoustic field $p(t, \mathbf{r})$ measured after passing the system characterised by scattering function $h(t, \mathbf{r})$, is related to transmitted acoustic field $g(t, \mathbf{r})$ via the integral equation [5]:

$$p(t, \mathbf{r}) = \int h(t - \tau, \mathbf{r}) \cdot g(\tau, \mathbf{r})\, d\tau. \tag{11}$$

If one is given $g(t, \mathbf{r})$ and $p(t, \mathbf{r})$ functions, the scattering function $h(t, \mathbf{r})$ can be obtained via direct or iterative inverse filtering techniques. However, if only time description $p(t)$ of a received acoustic pressure field $p(t, \mathbf{r})$ is available (in a form of the echo envelope), a special model of sound scattering on a rough bottom surface will be helpful for obtaining the bottom scattering function $h(t, \mathbf{r})$.

7. Conclusion

The results of the presented investigation are promising, as they show that evaluation of the fractal dimension of acoustic echo signal scattered at the seabed may be a useful simple (single- or two- parameter) method of bottom typing. The results are not worse than those obtained concurrently using other methods. The fractal box dimension method when combined with other parameters of bottom echo envelope can add useful information and improve the reliability of sea bottom typing. However, it must be noticed that the data used in paper were acquired only from relatively small water region, so the method should be verified for a larger area and for different bottom types.

The developed method was implemented (among other methods) in Visual Bottom Typer [8] – the computerized system for the seabed identification and imaging, developed in Acoustics Department, Technical University of Gdask, in co-operation with BioSonics Inc. In this system fractal dimension method is combined with the technique based on the first echo energy division [1]. The data points are plotted in the (E_1, D_{box}) space in run time and the bottom type is assigned referring to regions in that space defined by user as shown in Fig. 7, similarly to Roxann method [3].

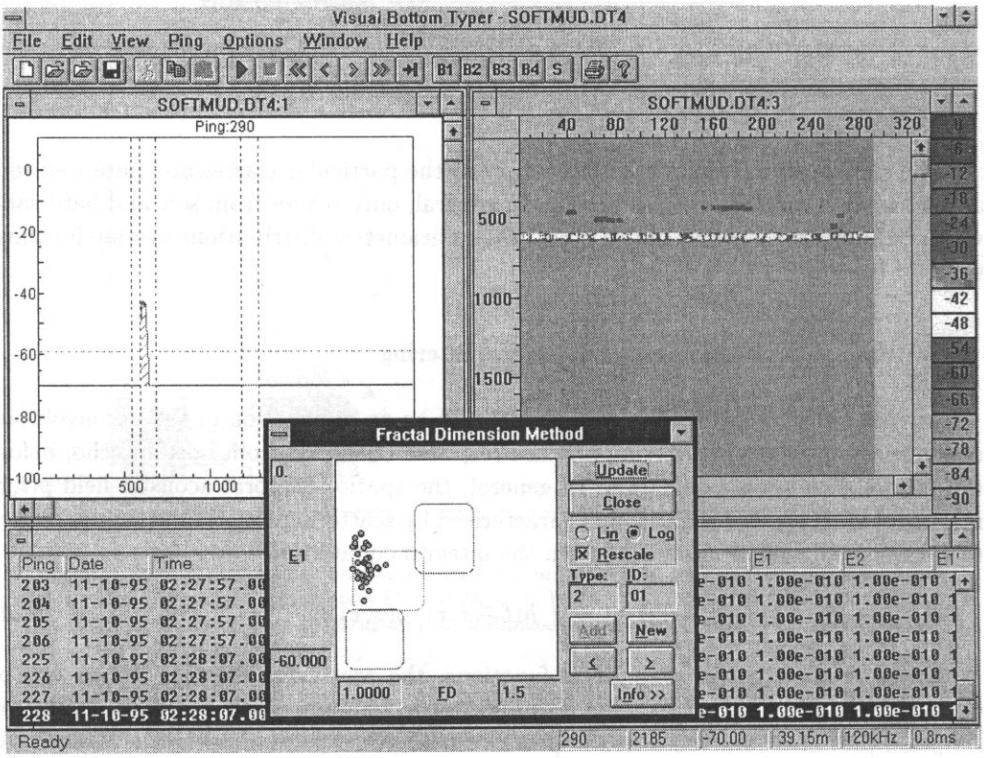

Fig. 7. Sample screen of VBT (Visual Bottom Typer) system for sea bed identification and imaging, with Fractal Dimension Method window.

References

[1] D. BAKIERA, A. STEPNOWSKI, *Method of the sea bottom classification with a division of the first echo signal*, Proceedings of the XIIIth Symposium on Hydroacoustics, Gdynia-Jurata, 55–60 (1996).

[2] L.R. LEBLANC, L. MAYER, M. RUFINO, S.G. SCHOCK, J. KING, *Marine sediment classification using the chirp sonar*, J. Acoust. Soc. Am., **91**, 1, 107–115 (1992).

[3] R.C. CHIVERS, *Acoustical sea-bed characterisation*, XIth Symposium on Hydroacoustics, Jurata (1994) [invited paper].

[4] M. GENSANE, H. TARAYRE, *Tests of sea-bottom discrimination with a parametric array*, Acoustic Letters, **16**, 5, 110–115 (1992).

[5] W.C. KNIGHT, R.G. PRIDHAM, S.M. KAY, *Digital signal processing for sonar*, Proc. IEEE, **69**, 11, 1451–1506 (1981).

[6] Z. ŁUBNIEWSKI, A. STEPNOWSKI, *Sea bottom typing using fractal dimension*, Proceedings of the International EAA/FASE Symposium on Hydroacoustics and Ultrasonics, Gdańsk-Jurata, 131–134 (1997).

[7] E. POULIQUEN, X. LURTON, *Sea-bed identification using echosounder signal*, European Conference on Underwater Acoustics, Elsevier Applied Science, London and New York, 535 (1992).

[8] A. STEPNOWSKI, M. MOSZYŃSKI, R. KOMENDARCZYK, J. BURCZYŃSKI, *Visual real-time Bottom Typing System (VBTS) and neural networks experiment for sea bed classification*, Proceedings of the 3rd European Conference on Underwater Acoustics, Heraklion, Crete, 685–690 (1996).

[9] H. M. HASTINGS, G. SUGIHARA, *Fractals. A user's guide for the natural sciences*, Oxford University Press, Oxford, New York, Tokyo (1994), pp. 7–77.

[10] K. JAJUGA, *Statistical theory of pattern recognition* [in Polish], PWN, Warszawa 1977, pp. 119–124.

[11] B.B. MANDELBROT, *The fractal geometry of nature*, Freeman, San Francisco 1982.

[12] *anon.*, Quester Tangent (1997), Quester Tangent Marine Instrumentation, 13 February 1997, http://www.questercorp.com/

[13] J. TĘGOWSKI, *Characteristic features of backscattering of the ultrasonic signals from the sea bottom at the Southern Baltic* [in Polish], Ph.D. Thesis, Institute of Oceanology of Polish Academy of Sciences, Sopot 1994.